Focusing of laser produced proton beams by using hemispherical targets

S Kar, M Borghesi, L Romagnani

Department of Pure and Applied Physics, Queen's University of Belfast, Belfast, BT7 1NN, UK

P K Patel, A J Mackinnon, R Snavely, M H Key

Lawrence Livermore National Laboratory, Livermore, CA 94551, USA

J A King, B Zhang, K U Akli

Department of Applied Science, University of California, Davis, CA 95616, USA

R R Freeman

Department of Physics, Ohio State University, Ohio, OH 43210, USA

R J Clarke, R Heathcote, D Neely

Central Laser Facility, CCLRC Rutherford Appleton Laboratory, Chilton, Didcot, Oxon., OX11 0QX, UK

Main contact email address: *s.kar@qub.ac.uk*

Introduction

The laboratory production of high density, uniformly heated plasma is a very useful tool for physical studies of interest to planetary and stellar astrophysics[1)] and fusion energy research[2)]. The production of plasmas with uniform density and temperature requires uniform heating on a time scale much shorter than the time required for significant hydrodynamic expansion. One possibility to achieve such an idealized state is via isochoric heating of solid-density matter with a short duration proton burst, such as the one produced from the rear side of thin foils irradiated by high-power lasers[3)].

Recently, this technique has been employed by Patel *et al.*[4)] and has been proven advantageous for this purpose.

The major issue with the proton beam generated from thin foils for this application is its divergence. It is very important to understand the degree of convergence of the proton beam emitted from the curved target, in order to optimize the target geometry for achieving maximum heating efficiency.

According to PIC simulations, carried out by several groups[5, 6)], the focus of the proton beam emitted from the hemispherical target is localized near the geometrical centre of the hemisphere. We report here on an experiment carried out at the Rutherford Appleton Laboratory employing a near-petawatt laser pulse, which has provided evidence of efficient isochoric heating of matter using the protons emitted from hemispherical targets. The size of the proton beam emitted from the hemispherical target, at a given energy, was measured at different positions by using secondary targets (to be heated isochorically) placed at different distances from the hemisphere. The data provides evidence of the proton beam divergence after reaching its focus, close to the geometrical focus of the hemisphere.

Experimental Setup

The experiment was carried out at the Vulcan Target Area Petawatt (TAP) of the Rutherford Appleton Laboratory. The CPA pulse delivered typically 250 Joule of energy onto target in 0.8 ps duration. Two different types of target assemblies were used in the experiment, in addition to single flat foils for preliminary investigations on proton generation. The first type (type-A) consists of two parallel thin flat foils separated by a certain distance. One of the two foils (the *proton target*) was irradiated by the laser pulse in order to produce the proton beam. The other foil (*secondary target*) was heated by the protons accelerated from the first foil. The second type (type-B) used in the experiment consisted of a hemispherical metal foil (the *proton target*) backed by a flat foil (*secondary target*).

During these measurements the CPA beam was focused, on the front side of the proton target, down to a spot of 80 µm diameter with peak intensity ~ 10^{18} W/cm^2. The purpose was to have a wider source of protons in order to sample effectively the curvature of the hemispherical target.

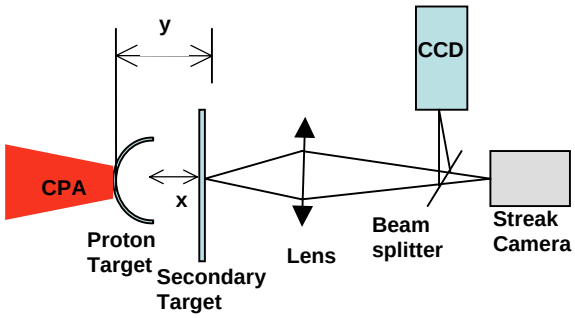

Figure 1. Schematic of the experimental setup using type-B target.

The optical emission at wavelength 527 nm from the rear side of the secondary target was simultaneously observed by an optical streak camera (IMACON 500 - S20), producing a time resolved picture and a 16 bit CCD camera producing a time integrated picture. Wavelength selection of the broadband Plankian emission from the heated target was done by using interference filters. The schematic of the set up is shown in Figure 1. The spatial resolution of the optical diagnostics was 10 µm and 8 µm for 527 nm and 400 nm respectively. The temporal resolution of the streak camera was set to 40 ps, which is much shorter than the time scale of hydrodynamic expansion of the hot region at the back of the secondary target. A transverse Nomarsky interferometer was used to diagnose the plasma produced at the targets' surfaces, at different times following the interaction. Particular attention was given to the plasma created at the rear side of the secondary target. The optical probe beam for the interferometer was generated by doubling the frequency of a very small portion of the main CPA beam. The delay of the probe beam was adjusted with ps resolution by a conventional double pass optical time slide.

Data Analysis

The flat foil target was used to obtain information about proton beam characteristics such as its source size, divergence and spectrum. Aiming for a straightforward measurement of the source size, we had tried flat foils having periodic grooves on the rear surface, motivated by the idea implemented by Cowan *et al.*[7)]. Unfortunately, the images of the grooves on the RCF were not so prominent to be used as univocal evidence. The second approach used, in order to obtain the source size, was to find out the position of the 'virtual' source size, as done by Borghesi *et al.*[8)] and the half-cone divergence angle of the proton beam, by looking at its size at different transverse planes.

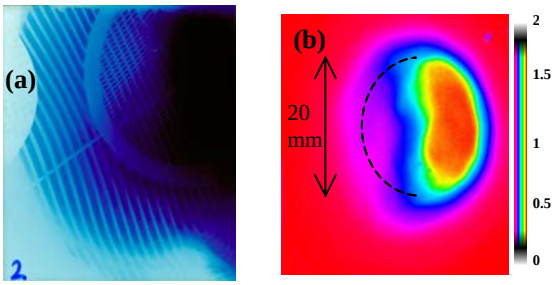

Figure 2. (a) The proton radiograph of two crossed parallel line meshes (400 LPI), placed at 2.06 mm and 4.06 mm after the target, observed over the RCF, placed at a distance of 5 cm from the target, corresponding to the proton energy of ~ 5.4 MeV. (b) 2D optical density profile over the RCF (in a separate shot) located at 5 cm from the target and exposed to the proton beam of energy ~ 5 MeV. The half circle intends to visualise the circular shape of the beam at half maximum of the optical density.

Figure 2(a) shows the radiograph of two crossed 400 lpi parallel line meshes, placed at different distances (2 mm and 4 mm) from the target, obtained by using protons of energy around 5.4 MeV originated from a 15 µm flat Au foil. From the calculation of the magnification for both meshes, $M=(L+x)/(l+x)$ where, L and l are the distances of the detector and mesh from the target rear surface, it was inferred that the virtual source is located at $x \approx 500$ µm behind the target. The FWHM of the beam has been estimated unambiguously from another shot obtained at similar irradiance, and with the same target and target-to-detector distance. The 2D optical density profile over the RCF (see Figure 2 (b)), where the dose is deposited mostly by protons of energy around 5 MeV, shows a semi-circular shape, of diameter 20 ± 2 mm at half maximum. The half circular pattern of the higher dose level is most likely due to the intensity variation across the laser spot on the target[9]. One can estimate the half cone angle divergence of the proton beam, of energy ≈ 5 MeV, as 11° ± 1° and the FWHM of its 'real' source at the rear of the target as 200 ± 20 µm. Information on the proton beam spectrum was also obtained. From the series of different shots, assuming an exponential spectrum, the proton beam has been found having temperature and cut-off energy of 3 MeV and 19 MeV respectively.

Before proceeding to the hemispherical targets, a few shots with target type-A were conducted in order to complete the preliminary investigations. A set of data obtained from a shot using target type-A is shown in Figure 3. In this case, a 15 µm Al foil was placed at a distance of 290 µm in front of the CPA irradiated 20 µm Al foil. The time integrated image of the source of radiation at the rear surface of the secondary target (Figure 3(b)), shows an overall circular shape of the heated region with FWHM diameter ~ 850 µm.

Since the temporal resolution of the optical streak camera (~ 40 ps) is much shorter than the time scale of hydrodynamic expansion, the initial bright spot in the streak of the optical emission from the secondary target contains, in principle, contributions from transition radiation processes. However, the intensity of the transition radiation is much less than the Plankian emission, as can be estimated by comparison with the transition radiation obtained in a series of measurements of rear surface emission from thin foils, irradiated at different irradiances. Therefore, the spatial dimension of the size of the streak at the initial time, in Figure 3(c) can be considered as the spatial extent of the proton heated area at the rear side of the secondary target. The interferogram taken at 400 ps, after the interaction of the CPA pulse (see Figure 3(a)), also shows the expanded plasma from a transverse area of ~ 300 ± 50 µm at the rear of the secondary target.

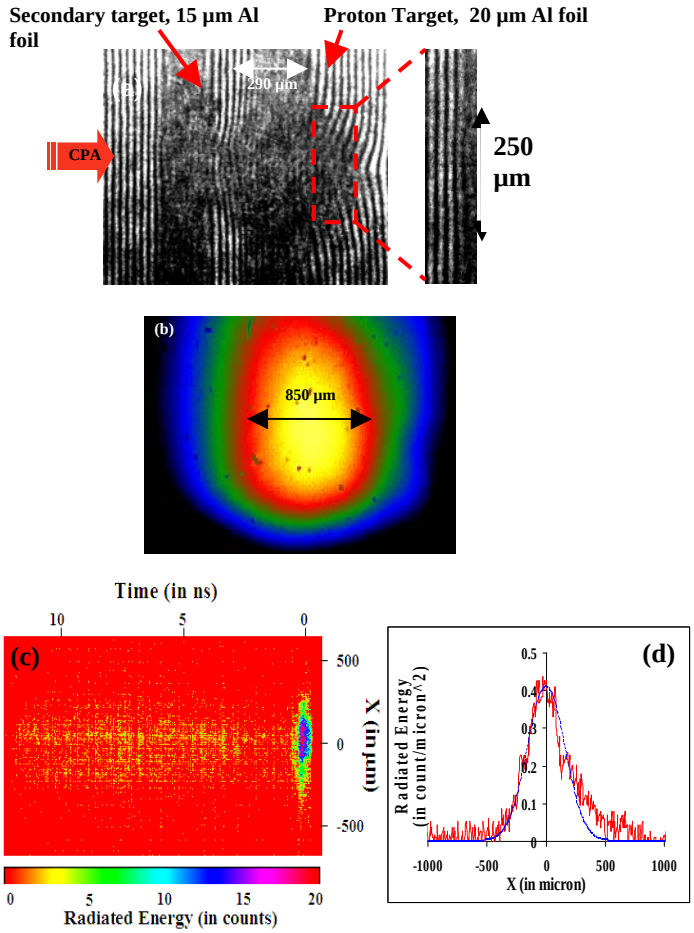

Figure 3. (a) The interferogram taken at 400 ps after the interaction of the CPA with target type - A. (b) The time integrated images of the optical emission from the rear surface of the secondary target (c) is the simultaneously taken time resolved image of the emission. The lineout (red) of radiated energy along the axis, t=0, is shown in (d), along with a Gaussian fit (blue dotted) of 370 µm FWHM.

The uniformly heated area of 370 µm FWHM, at the rear surface of a secondary foil, obtained from the time resolved image, can be mapped to a proton source of FWHM of 230 µm at the rear surface of the proton target, taking into account the estimation for the location of the virtual source of protons obtained from the analysis of proton radiographs of meshes. This estimation of the 'real' source size also agrees with the one obtained from the analysis of the proton radiographs.

Sets of data were obtained using target type-B, where the thickness and the position of the secondary foil were varied. Figure 4 shows the time resolved and time integrated images of the optical emission from the back of the secondary target, obtained for three different configurations. Several interesting effects are observed. From the comparison between the time resolved images in Figure 3(c) with the respective images in Figure 4(a) [where the only difference is the shape of the proton target], we observed a reduction of a factor of 2.75 in the spatial extent (equivalent to reduction of area of heated region by a factor of 7.5) of the heated region in the latter case, along with an increase of a factor of 6.5 in the peak energy flux of emission. This provides strong evidence of ballistic focusing of the proton beam and enhancement in the temperature of the isochorically heated matter.

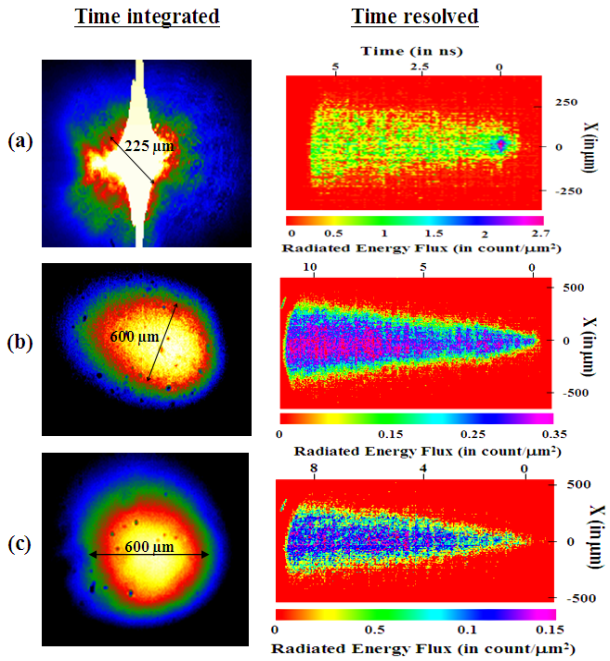

Figure 4. The images obtained (at 527 nm) from type-B targets having the thickness of secondary target (Al foil) and 'x'(see Figure 1) as (a) 15 µm, 0 µm (b) 15 µm, 100µm and (c) 100 µm, 0 µm respectively. The proton target was 15 µm Al hemispheres of diameter of 440 µm. The color scales of the images are different for different time integrated images.

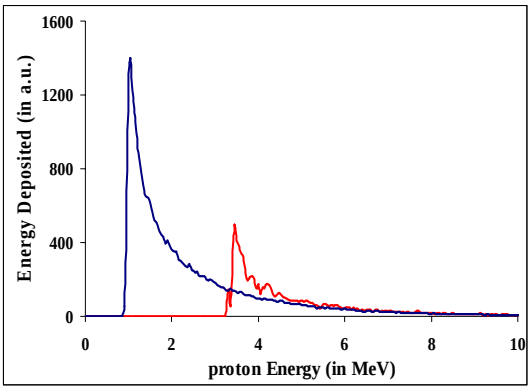

Figure 5. Energy deposited by protons of different energy, having a Maxwell-Boltzmann spectrum of 3 MeV temperature, in the last 2 µm thick layer (arbitrarily selected) of Al foil of 15 µm (blue) and 100 µm (red) thickness.

Secondly, it has been observed that the FWHM of the heated region at the rear surface of the secondary target does not change significantly with its thickness, when the distance of the rear surface of the secondary target from the hemisphere remains the same (see Figure 4(b) and 4(c)). An interesting point in these two images is that in the case of a 100 µm thick secondary foil, the peak energy flux of the optical emission is 27% of that in the other case. This variation correlates well with the computed energy deposition by a proton beam of expected parameters, using the Monte Carlo simulation, TRIM [10]. Considering a proton beam spectrum obeying Maxwell-Boltzmann statistics with a temperature of 3 MeV, the total energy deposited by protons in, say, a 2 µm thick layer (thickness arbitrarily chosen as an example) at the rear of 100 µm thick Al foil is 34% of that released in a layer of the same thickness at the rear of 15 µm Al foil (Figure 5).

Finally, further information achieved from the experiment is the increase in the FWHM of the heated region, when the distance of the back surface of the secondary target from the geometrical centre of the hemispherical target increases, irrespective of the thickness of the secondary target, as shown in Figure 6. The minimum FWHM of the heated region was observed when the back of the secondary target was close to the geometrical centre of the hemisphere and was less than the expected FWHM of the source of proton beam emerging from the back of the hemisphere. This suggests that the proton beam from the inner surface of the hemisphere attains minimum size at some point in the close proximity of the geometrical centre of the hemisphere.

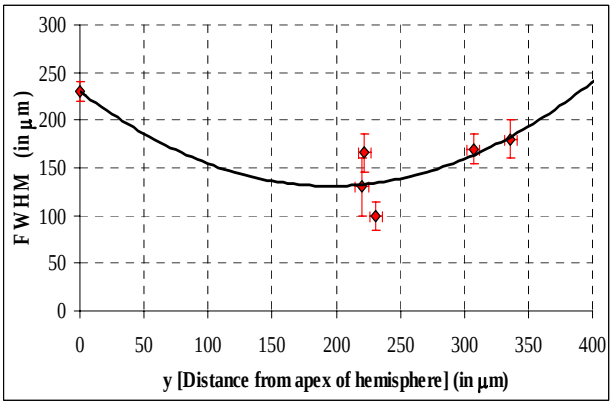

Figure 6. The size of the proton heated area at the back of the secondary target versus its distance from the apex of the hemispherical proton target, obtained from different shots. The value of ordinate at y=0 is the real source size (for 5 MeV protons) estimated from the shot using type-A target. The black solid line is a second order polynomial fit of the data points.

Conclusion

The focusing effect of proton beams produced via high power laser thin foil interaction has been observed by employing hemispherical targets. This is observed experimentally by looking at the optical emission from secondary targets isochorically heated by the proton beams originated from the hemispherical targets. The gradual increase of the emission source size after the geometrical focus of the hemispherical targets suggests that the focal plane of the proton beam is located in close proximity to the geometrical centre of the hemispherical target.

References

1. B.A. Remington, *et al.*, Science, 284, 1488 (1999)
2. J. Nuckolls, *et al.*, Nature, 239, 139 (15)
3. R.A. Snavely, *et al.*, Phys. Rev. Lett., 85, 2945 (2000)
4. P.K. Patel, *et al.*, Phys. Rev. Lett., 91, 125004 (2003)
5. S.C. Wilks, *et al.*, Phys Plasmas, 8, 542 (2001)
6. H. Ruhl, *et al.*, Plasma Physics Reports, 27, 363 (2001)
7. T.E. Cowan, *et al.*, Phys. Rev. Lett., 92, 204801 (2004)
8. M. Borghesi, *et al.*, Phys. Rev. Lett., 92, 55003 (2004)
9. J. Fuchs, *et al.*, Phys. Rev. Lett., 91, 255002 (2003)
10. www.srim.org